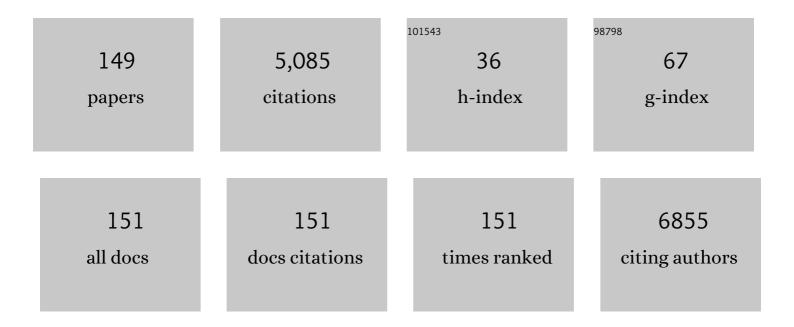
Keiji Ueno

List of Publications by Year in descending order

Source: https://exaly.com/author-pdf/5046104/publications.pdf Version: 2024-02-01



KEUL LIENO

#	Article	IF	CITATIONS
1	Ambipolar MoTe ₂ Transistors and Their Applications in Logic Circuits. Advanced Materials, 2014, 26, 3263-3269.	21.0	388
2	Large-Area Synthesis of High-Quality Uniform Few-Layer MoTe ₂ . Journal of the American Chemical Society, 2015, 137, 11892-11895.	13.7	302
3	Strong Enhancement of Raman Scattering from a Bulk-Inactive Vibrational Mode in Few-Layer MoTe ₂ . ACS Nano, 2014, 8, 3895-3903.	14.6	275
4	High-performance top-gated monolayer SnS2 field-effect transistors and their integrated logic circuits. Nanoscale, 2013, 5, 9666.	5.6	269
5	Self-Limiting Layer-by-Layer Oxidation of Atomically Thin WSe ₂ . Nano Letters, 2015, 15, 2067-2073.	9.1	204
6	Flat bands in twisted bilayer transition metal dichalcogenides. Nature Physics, 2020, 16, 1093-1096.	16.7	197
7	Self-Limiting Oxides on WSe ₂ as Controlled Surface Acceptors and Low-Resistance Hole Contacts. Nano Letters, 2016, 16, 2720-2727.	9.1	131
8	Synthesis of Highâ€Quality Largeâ€Area Homogenous 1T′ MoTe ₂ from Chemical Vapor Deposition. Advanced Materials, 2016, 28, 9526-9531.	21.0	125
9	Heteroepitaxial growth of layered transition metal dichalcogenides on sulfurâ€ŧerminated GaAs{111} surfaces. Applied Physics Letters, 1990, 56, 327-329.	3.3	113
10	Electrostatically Reversible Polarity of Ambipolar α-MoTe ₂ Transistors. ACS Nano, 2015, 9, 5976-5983.	14.6	113
11	Monolayer 1T-NbSe2 as a Mott insulator. NPG Asia Materials, 2016, 8, e321-e321.	7.9	109
12	Epitaxial growth of transition metal dichalcogenides on cleaved faces of mica. Journal of Vacuum Science and Technology A: Vacuum, Surfaces and Films, 1990, 8, 68-72.	2.1	108
13	Accumulation and Depletion Layer Thicknesses in Organic Field Effect Transistors. Japanese Journal of Applied Physics, 2003, 42, L1408-L1410.	1.5	105
14	Highly efficient crystalline silicon/Zonyl fluorosurfactant-treated organic heterojunction solar cells. Applied Physics Letters, 2012, 100, .	3.3	102
15	Double resonance Raman modes in monolayer and few-layer <mml:math xmlns:mml="http://www.w3.org/1998/Math/MathML"><mml:msub><mml:mi mathvariant="normal">MoTe<mml:mn>2</mml:mn></mml:mi </mml:msub>. Physical Review B. 2015. 91</mml:math 	3.2	99
16	Twist Angle-Dependent Interlayer Exciton Lifetimes in van der Waals Heterostructures. Physical Review Letters, 2021, 126, 047401.	7.8	88
17	Highly Efficient Solutionâ€Processed Poly(3,4â€ethylenedioâ€xythiophene):Poly(styrenesulfonate)/Crystalline–Silicon Heterojunction Solar Cells with Improved Lightâ€Induced Stability. Advanced Energy Materials, 2015, 5, 1500744.	19.5	85
18	Application of Van der Waals epitaxy to highly heterogeneous systems. Journal of Crystal Growth, 1989, 95, 603-606.	1.5	80

#	Article	lF	CITATIONS
19	Heteroepitaxial growth by Van der Waals interaction in one-, two- and three-dimensional materials. Journal of Crystal Growth, 1991, 111, 1029-1032.	1.5	74
20	Origin of Noise in Layered MoTe ₂ Transistors and its Possible Use for Environmental Sensors. Advanced Materials, 2015, 27, 6612-6619.	21.0	72
21	Carrier Polarity Control in α-MoTe ₂ Schottky Junctions Based on Weak Fermi-Level Pinning. ACS Applied Materials & Interfaces, 2016, 8, 14732-14739.	8.0	72
22	Reversible and Precisely Controllable p/nâ€Type Doping of MoTe ₂ Transistors through Electrothermal Doping. Advanced Materials, 2018, 30, e1706995.	21.0	68
23	Heteroepitaxy of Layered Semiconductor GaSe on a GaAs(111)B Surface. Japanese Journal of Applied Physics, 1991, 30, L1352-L1354.	1.5	63
24	Nafion-Modified PEDOT:PSS as a Transparent Hole-Transporting Layer for High-Performance Crystalline-Si/Organic Heterojunction Solar Cells with Improved Light Soaking Stability. ACS Applied Materials & Interfaces, 2016, 8, 31926-31934.	8.0	63
25	Heteroepitaxial Growth of Layered Semiconductor GaSe on a Hydrogen-Terminated Si(111) Surface*. Japanese Journal of Applied Physics, 1993, 32, L434-L437.	1.5	47
26	Construction of van der Waals magnetic tunnel junction using ferromagnetic layered dichalcogenide. Applied Physics Letters, 2015, 107, .	3.3	47
27	Correlation between the fine structure of spin-coated PEDOT:PSS and the photovoltaic performance of organic/crystalline-silicon heterojunction solar cells. Journal of Applied Physics, 2016, 120, .	2.5	46
28	Sensitive Phonon-Based Probe for Structure Identification of 1T′ MoTe ₂ . Journal of the American Chemical Society, 2017, 139, 8396-8399.	13.7	46
29	Bulk heterojunction organic photovoltaic cell fabricated by the electrospray deposition method using mixed organic solvent. Physica Status Solidi - Rapid Research Letters, 2011, 5, 229-231.	2.4	45
30	Optical anisotropy in solvent-modified poly(3,4-ethylenedioxythiophene):poly(styrenesulfonic acid) and its effect on the photovoltaic performance of crystalline silicon/organic heterojunction solar cells. Applied Physics Letters, 2013, 102, .	3.3	43
31	Anisotropic band splitting in monolayer NbSe2: implications for superconductivity and charge density wave. Npj 2D Materials and Applications, 2018, 2, .	7.9	43
32	Self-passivated ultra-thin SnS layers <i>via</i> mechanical exfoliation and post-oxidation. Nanoscale, 2018, 10, 22474-22483.	5.6	42
33	Exfoliation and van der Waals heterostructure assembly of intercalated ferromagnet Cr _{1/3} TaS ₂ . 2D Materials, 2017, 4, 041007.	4.4	41
34	2D Tunnel Field Effect Transistors (FETs) with a Stable Chargeâ€Transferâ€Type p ⁺ â€WSe ₂ Source. Advanced Electronic Materials, 2018, 4, 1800207.	5.1	41
35	Molecular Layer-by-Layer Growth of C ₆₀ Thin Films by Continuous-Wave Infrared Laser Deposition. Applied Physics Express, 2008, 1, 015005.	2.4	39
36	Pronounced photogating effect in atomically thin WSe2 with a self-limiting surface oxide layer. Applied Physics Letters, 2018, 112, .	3.3	38

#	Article	IF	CITATIONS
37	Introduction to the Growth of Bulk Single Crystals of Two-Dimensional Transition-Metal Dichalcogenides. Journal of the Physical Society of Japan, 2015, 84, 121015.	1.6	36
38	Changes in structure and chemical composition of α-MoTe ₂ and β-MoTe ₂ during heating in vacuum conditions. Applied Physics Express, 2015, 8, 095201.	2.4	36
39	All 2D Heterostructure Tunnel Field-Effect Transistors: Impact of Band Alignment and Heterointerface Quality. ACS Applied Materials & Interfaces, 2020, 12, 51598-51606.	8.0	35
40	Investigation of the growth mechanism of layered semiconductor GaSe. Applied Surface Science, 1997, 113-114, 38-42.	6.1	34
41	Fabrication of Transparent and Flexible Organic Field-Effect Transistors with Solution-Processed Graphene Source–Drain and Gate Electrodes. Applied Physics Express, 2011, 4, 021603.	2.4	31
42	Green-tea modified multiwalled carbon nanotubes for efficient poly(3,4-ethylenedioxythiophene):poly(stylenesulfonate)/n-silicon hybrid solar cell. Applied Physics Letters, 2013, 102, .	3.3	31
43	Hetero-epitaxy of layered compound semiconductor GaSe onto GaAs surfaces for very effective passivation of nanometer structures. Surface Science, 1992, 267, 43-46.	1.9	30
44	Origin of the ambipolar operation of a pentacene field-effect transistor fabricated on a poly(vinyl) Tj ETQq0 0 0 94, 083305.	rgBT /Over 3.3	lock 10 Tf 50 29
45	Gate-Tunable Thermal Metal–Insulator Transition in VO ₂ Monolithically Integrated into a WSe ₂ Field-Effect Transistor. ACS Applied Materials & Interfaces, 2019, 11, 3224-3230.	8.0	29
46	Investigation of the growth mechanism of an InSe epitaxial layer on a MoS2 substrate. Journal of Crystal Growth, 2000, 219, 115-122.	1.5	28
47	Efficient Crystalline Si/Poly(ethylene dioxythiophene):Poly(styrene sulfonate):Graphene Oxide Composite Heterojunction Solar Cells. Applied Physics Express, 2012, 5, 032301.	2.4	28
48	Ultrathin Bismuth Film on 1T-TaS ₂ : Structural Transition and Charge-Density-Wave Proximity Effect. Nano Letters, 2018, 18, 3235-3240.	9.1	28
49	In-situ measurement of molecular orientation of the pentacene ultrathin films grown on SiO2 substrates. Surface Science, 2006, 600, 2518-2522.	1.9	27
50	Anodization of electrolytically polished Ta surfaces for enhancement of carrier injection into organic field-effect transistors. Journal of Applied Physics, 2005, 98, 114503.	2.5	26
51	Barium hydroxide hole blocking layer for front- and back-organic/crystalline Si heterojunction solar cells. Journal of Applied Physics, 2017, 122, .	2.5	26
52	lonic liquid-mediated epitaxy of high-quality C60 crystallites in a vacuum. CrystEngComm, 2012, 14, 4939.	2.6	24
53	Improved photovoltaic performance of crystalline-Si/organic Schottky junction solar cells using ferroelectric polymers. Applied Physics Letters, 2013, 103, .	3.3	24
54	Bulk-like pentacene epitaxial films on hydrogen-terminated Si(111). Applied Physics Letters, 2005, 87, 061917.	3.3	23

#	Article	IF	CITATIONS
55	Chemical mist deposition of graphene oxide and PEDOT:PSS films for crystalline Si/organic heterojunction solar cells. Physica Status Solidi C: Current Topics in Solid State Physics, 2012, 9, 2134-2137.	0.8	22
56	Effects of molybdenum oxide molecular doping on the chemical structure of poly(3,4-ethylenedioxythiophene):poly(stylenesulfonate) and on carrier collection efficiency of silicon/poly(3,4-ethylenedioxythiophene):poly(stylenesulfonate) heterojunction solar cells. Applied Physics Letters, 2013, 102, 183503.	3.3	22
57	Ultrafast dynamics of the low frequency shear phonon in 1T′-MoTe2. Applied Physics Letters, 2020, 116, .	3.3	21
58	Fabrication and Surface Engineering of Two-Dimensional SnS Toward Piezoelectric Nanogenerator Application. MRS Advances, 2018, 3, 2809-2814.	0.9	19
59	Nanostructure fabrication by selective growth of molecular crystals on layered material substrates. Applied Physics Letters, 1997, 70, 1104-1106.	3.3	18
60	Efficient organic/polycrystalline silicon hybrid solar cells. Nano Energy, 2015, 11, 260-266.	16.0	18
61	Self-assembled silver nanowires as top electrode for poly(3,4-ethylenedioxythiophene):poly(stylenesulfonate)/n-silicon solar cell. Thin Solid Films, 2014, 558, 306-310.	1.8	16
62	Investigating the chemical mist deposition technique for poly(3,4-ethylenedioxythiophene):poly(styrene sulfonate) on textured crystalline-silicon for organic/crystalline-silicon heterojunction solar cells. Japanese Journal of Applied Physics, 2016, 55, 031601.	1.5	16
63	Material and Device Structure Designs for 2D Memory Devices Based on the Floating Gate Voltage Trajectory. ACS Nano, 2021, 15, 6658-6668.	14.6	16
64	A Novel Method to Fabricate a Molecular Quantum Structure: Selective Growth of C60on Layered Material Heterostructures. Japanese Journal of Applied Physics, 1999, 38, 511-514.	1.5	15
65	Highly sensitive reflection high-energy electron diffraction measurement by use of micro-channel imaging plate. Review of Scientific Instruments, 2000, 71, 3478-3479.	1.3	15
66	Step-bunched Bi-terminated Si(111) surfaces as a nanoscale orientation template for quasisingle crystalline epitaxial growth of thin film phase pentacene. Applied Physics Letters, 2008, 93, 223303.	3.3	15
67	Solution-processed crystalline silicon double-heterojunction solar cells. Applied Physics Express, 2016, 9, 022301.	2.4	15
68	Improved efficiency of methylammonium-free perovskite thin film solar cells by fluorinated ammonium iodide treatment. Organic Electronics, 2020, 78, 105596.	2.6	15
69	Heteroepitaxial Growth of Layered GaSe Films on GaAs(001) Surfaces. Japanese Journal of Applied Physics, 1993, 32, L1444-L1447.	1.5	14
70	Fabrication of GaAs Quantum Dots on a Bilayer-GaSe Terminated Si(111) Substrate. Japanese Journal of Applied Physics, 2001, 40, 1888-1891.	1.5	13
71	Optical properties and carrier transport in c-Si/conductive PEDOT:PSS(GO) composite heterojunctions. Physica Status Solidi C: Current Topics in Solid State Physics, 2012, 9, 2075-2078.	0.8	13
72	Oxygen-Sensitive Layered MoTe ₂ Channels for Environmental Detection. ACS Applied Materials & Interfaces, 2019, 11, 47047-47053.	8.0	13

#	Article	IF	CITATIONS
73	Low-Energy Electron Energy Loss Spectroscopy on YBa2Cu3O7-y. Japanese Journal of Applied Physics, 1988, 27, L304-L307.	1.5	12
74	Visible light photoemission and negative electron affinity of single-crystalline CsCl thin films. Surface Science, 2003, 544, 220-226.	1.9	12
75	Atmospheric-pressure argon plasma etching of spin-coated 3,4-polyethylenedioxythiophene:polystyrenesulfonic acid (PEDOT:PSS) films for cupper phtalocyanine (CuPc)/C60 heterojunction thin-film solar cells. Thin Solid Films, 2011, 519, 6834-6839.	1.8	12
76	Role of Isopropyl Alcohol Solvent in the Synthesis of Organic–Inorganic Halide CH(NH ₂) ₂ PbI _{<i>x</i>} Br _{3–<i>x</i>} Perovskite Thin Films by a Two-Step Method. Journal of Physical Chemistry C, 2016, 120, 25371-25377.	3.1	12
77	Exciton diffusion in <mml:math xmlns:mml="http://www.w3.org/1998/Math/MathML"> <mml:mrow> <mml:mi>h </mml:mi> <mml:mi>BN </mml:mi> -encapsulated monolayer <mml:math xmlns:mml="http://www.w3.org/1998/Math/MathML"> <mml:mrow> <mml:mi>Mo </mml:mi> <mml:msub> <mml:m< td=""><td>3.2</td><td>12</td></mml:m<></mml:msub></mml:mrow></mml:math </mml:mrow></mml:math 	3.2	12
78	Physical Review 6, 2020, 2027. Methyl-terminated Si(111) surface as the ultra thin protection layer to fabricate position-controlled alkyl SAMs by using atomic force microscope anodic oxidation. Surface Science, 2004, 552, 46-52.	1.9	11
79	Nanotransfer of the Polythiophene Molecular Alignment onto the Step-Bunched Vicinal Si(111) Substrate. Langmuir, 2008, 24, 11605-11610.	3.5	11
80	Efficient Organic Photovoltaic Cells Using Hole-Transporting MoO3Buffer Layers Converted from Solution-Processed MoS2Films. Japanese Journal of Applied Physics, 2011, 50, 071604.	1.5	11
81	Understanding the Memory Window Overestimation of 2D Materials Based Floating Gate Type Memory Devices by Measuring Floating Gate Voltage. Small, 2020, 16, e2004907.	10.0	11
82	Investigation of laser-induced-metal phase of MoTe ₂ and its contact property via scanning gate microscopy. Nanotechnology, 2020, 31, 205205.	2.6	11
83	Quantitative Determination of Contradictory Bandgap Values of Bulk PdSe ₂ from Electrical Transport Properties. Advanced Functional Materials, 2022, 32, 2108061.	14.9	11
84	Characteristic Secondary Electron Emission from Graphite and Glassy Carbon Surfaces. Japanese Journal of Applied Physics, 1988, 27, L759-L761.	1.5	10
85	Nanostructure Fabrication Using Selective Growth on Nanosize Patterns Drawn by a Scanning Probe Microscope. Japanese Journal of Applied Physics, 1997, 36, 4061-4064.	1.5	10
86	Fabrication of an Organic Field-effect Transistor on a Mica Gate Dielectric. Chemistry Letters, 2006, 35, 354-355.	1.3	10
87	Photoâ€Induced Tellurium Segregation in MoTe ₂ . Physica Status Solidi - Rapid Research Letters, 2022, 16, .	2.4	10
88	Nano-scale anodic oxidation on a Si() surface terminated by bilayer-GaSe. Surface Science, 2002, 514, 27-32.	1.9	9
89	Effect of Organic Buffer Layer on Performance of Pentacene Field-Effect Transistor Fabricated on Natural Mica Gate Dielectric. Japanese Journal of Applied Physics, 2007, 46, L913-L916.	1.5	9
90	Real-time measurement of optical anisotropy during film growth using a chemical mist deposition of poly(3,4-ethylenedioxythiophene):poly(styrenesulfonate). Journal of Applied Physics, 2014, 115, 123514.	2.5	9

#	Article	IF	CITATIONS
91	Barrier Formation at the Contacts of Vanadium Dioxide and Transition-Metal Dichalcogenides. ACS Applied Materials & Interfaces, 2019, 11, 36871-36879.	8.0	9
92	Enhanced Exciton–Exciton Collisions in an Ultraflat Monolayer MoSe ₂ Prepared through Deterministic Flattening. ACS Nano, 2021, 15, 1370-1377.	14.6	9
93	Preparation of GaS Thin Films by Molecular Beam Epitaxy. Japanese Journal of Applied Physics, 1996, 35, L568-L570.	1.5	8
94	Efficient crystalline Si/organic hybrid heterojunction solar cells. Physica Status Solidi C: Current Topics in Solid State Physics, 2012, 9, 2101-2106.	0.8	8
95	Real-time ellipsometric characterization of the initial growth stage of poly(3,4-ethylenedioxythiophene):poly(styrene sulfonate) films by electrospray deposition using N,N-dimethylformamide solvent solution. Journal of Non-Crystalline Solids, 2012, 358, 2520-2524.	3.1	8
96	Effect of substrate bias on mist deposition of conjugated polymer on textured crystallineâ€ S i for efficient câ€ S i/organic heterojunction solar cells. Physica Status Solidi (A) Applications and Materials Science, 2016, 213, 1922-1925.	1.8	8
97	Intrinsic Electronic Transport Properties and Carrier Densities in PtS ₂ and SnSe ₂ : Exploration of n ⁺ â€Source for 2D Tunnel FETs. Advanced Electronic Materials, 2021, 7, 2100292.	5.1	8
98	Scanning Tunneling Microscope Observation of the Metal-Adsorbed Layered Semiconductor Surfaces. Japanese Journal of Applied Physics, 1995, 34, 3342-4445.	1.5	7
99	Fabrication of C60 nanostructures by selective growth on GaSe/MoS2 and InSe/MoS2 heterostructure substrates. Applied Surface Science, 1998, 130-132, 670-675.	6.1	7
100	Anisotropic Polymerization of a Long-Chain Diacetylene Derivative Langmuirâ^'Blodgett Film on a Step-Bunched SiO2/Si Surface. Langmuir, 2006, 22, 5742-5747.	3.5	7
101	Nucleation on the substrate surfaces during liquid flux-mediated vacuum deposition of rubrene. Journal of Crystal Growth, 2008, 311, 163-166.	1.5	7
102	Real-Time Ellipsometric Characterization of Initial Growth Stage of Poly(3,4-ethylene) Tj ETQq0 0 0 rgBT /Overlock Applied Physics, 2011, 50, 081603.	10 Tf 50 1.5	307 Td (diox 7
103	Improved performance of poly(3,4-ethylenedioxythiophene):poly(stylene sulfonate)/n-Si hybrid solar cell by incorporating silver nanoparticles. Japanese Journal of Applied Physics, 2014, 53, 110305.	1.5	7
104	Self assembled silver nanowire mesh as top electrode for organic–inorganic hybrid solar cell. Canadian Journal of Physics, 2014, 92, 867-870.	1.1	7
105	Fabrication of [CH(NH ₂) ₂] _{0.8} Cs _{0.2} PbI ₃ Perovskite Thin Films for n-i-p Planar-structure Solar Cells by a One-step Method Using 1-Cyclohexyl-2-pyrrolidone as an Additive. Chemistry Letters, 2018, 47, 905-908.	1.3	7
106	Highly crystalline large-grained perovskite films using two additives without an antisolvent for high-efficiency solar cells. Thin Solid Films, 2019, 679, 27-34.	1.8	7
107	Electrospray-Deposited Poly(3,4-ethylenedioxythiophene):Poly(styrene sulfonate) for Poly(3-hexylthiophene):Phenyl-C\$_{61}\$-Butyric Acid Methyl Ester Photovoltaic Cells. Japanese Journal of Applied Physics, 2012, 51, 10NE30.	1.5	6
108	Selective oxidation of the surface layer of bilayer WSe ₂ by laser heating. Japanese Journal of Applied Physics, 2019, 58, 120903.	1.5	6

Keiji Ueno

#	Article	IF	CITATIONS
109	Self-assembled Fluorinated Polymer Passivation Layer for Efficient Perovskite Thin-film Solar Cells. Chemistry Letters, 2020, 49, 87-90.	1.3	6
110	Mist chemical vapor deposition of crystalline MoS ₂ atomic layer films using sequential mist supply mode and its application in field-effect transistors. Nanotechnology, 2022, 33, 045601.	2.6	6
111	Reversible Chargeâ€Polarity Control for Multioperationâ€Mode Transistors Based on van der Waals Heterostructures. Advanced Science, 2022, 9, .	11.2	6
112	Electrospray Deposition of Poly(3-hexylthiophene) Films for Crystalline Silicon/Organic Hybrid Junction Solar Cells. Japanese Journal of Applied Physics, 2012, 51, 061602.	1.5	5
113	Fabrication of {CH(NH ₂) ₂ } _{1a^^} <i>_x</i> Cs <i>_x</i> PbI _{3<!--<br-->Perovskite Thin Films by Two-step Method and Its Application to Thin Film Solar Cells. Chemistry Letters. 2017. 46, 612-615.}	sup>	5
114	Crystalline Silicon/Graphene Oxide Hybrid Junction Solar Cells. Japanese Journal of Applied Physics, 2012, 51, 10NE22.	1.5	5
115	Electron-energy-loss spectroscopy of KxC60 and K-halides: comparison in the K3p excitation region. Applied Surface Science, 2001, 169-170, 184-187.	6.1	4
116	Efficient Organic Photovoltaic Cells Using MoO3Hole-Transporting Layers Prepared by Simple Spin-Cast of Its Dispersion Solution in Methanol. Japanese Journal of Applied Physics, 2013, 52, 020202.	1.5	4
117	Optical and carrier transport properties of graphene oxide based crystalline-Si/organic Schottky junction solar cells. Journal of Applied Physics, 2013, 114, .	2.5	4
118	Optical Anisotropy and Compositional Ratio of Conductive Polymer PEDOT:PSS and Their Effect on Photovoltaic Performance of Crystalline Silicon/Organic Heterojunction Solar Cells. , 2018, , 137-159.		4
119	Low-temperature growth of crystalline tungsten disulfide thin films by using organic liquid precursors. Japanese Journal of Applied Physics, 2020, 59, SCCC04.	1.5	4
120	Facile and Reversible Carrier-Type Manipulation of Layered MoTe ₂ Toward Long-Term Stable Electronics. ACS Applied Materials & Interfaces, 2020, 12, 42918-42924.	8.0	4
121	Synthesis of AlO <i>x</i> thin films by atmospheric-pressure mist chemical vapor deposition for surface passivation and electrical insulator layers. Journal of Vacuum Science and Technology A: Vacuum, Surfaces and Films, 2020, 38, .	2.1	4
122	AlO _{<i>x</i>} Thin Films Synthesized by Mist Chemical Vapor Deposition, Monitored by a Fast-Scanning Mobility Particle Analyzer, and Applied as a Gate Insulating Layer in the Field-Effect Transistors. ACS Applied Electronic Materials, 2021, 3, 658-667.	4.3	4
123	Electrospray Deposition of Poly(3-hexylthiophene) Films for Crystalline Silicon/Organic Hybrid Junction Solar Cells. Japanese Journal of Applied Physics, 2012, 51, 061602.	1.5	4
124	Real-Time Ellipsometric Characterization of the Initial Growth Stage of Poly(3,4-ethylene) Tj ETQq0 0 0 rgBT /Overl and Nanotechnology, 2011, 11, 8030-8034.	lock 10 Tf 0.9	50 147 Td (4
125	Ultrafast Operation of 2D Heterostructured Nonvolatile Memory Devices Provided by the Strong Short-Time Dielectric Breakdown Strength of <i>h</i> BN. ACS Applied Materials & Interfaces, 2022, 14, 25659-25669.	8.0	4
126	Scanning Tunneling Microscopy and Spectroscopy Study of LiBr/Si(001) Heterostructure. Japanese Journal of Applied Physics, 2004, 43, L203-L205.	1.5	3

#	Article	IF	CITATIONS
127	Orientation Control of Standing Epitaxial Pentacene Monolayers Using Surface Steps and In-plane Band Dispersion Analysis by Angle Resolved Photoelectron Spectroscopy. Materials Research Society Symposia Proceedings, 2006, 965, 1.	0.1	3
128	Depth profile characterization of spin-coated poly(3,4-ethylenedioxythiophene): poly(styrene sulfonic) Tj ETQq0 0 State Physics, 2011, 8, 3025-3028.	0 rgBT /C 0.8	verlock 10 ⁻ 3
129	Effect of thermally annealed atomic-layer-deposited AlOx/chemical tunnel oxide stack layer at the PEDOT:PSS/n-type Si interface to improve its junction quality. Journal of Applied Physics, 2020, 128, 045305.	2.5	3
130	Electrospray-Deposited Poly(3,4-ethylenedioxythiophene):Poly(styrene sulfonate) for Poly(3-hexylthiophene):Phenyl-C61-Butyric Acid Methyl Ester Photovoltaic Cells. Japanese Journal of Applied Physics, 2012, 51, 10NE30.	1.5	3
131	Structure of Organic Thin Films Grown on Surface-modified Tantalum Oxide. Chemistry Letters, 2006, 35, 746-747.	1.3	2
132	Depth Profile Characterization of Spin-Coated Poly(3,4-ethylenedioxythiophene):Poly(styrene sulfonic) Tj ETQq0 0 Japanese Journal of Applied Physics, 2011, 50, 08JG02.	0 rgBT /0 1.5	Overlock 10 2
133	Top-Contacted Organic Field-Effect Transistors with Graphene Electrodes Prepared by Laminate Transfer Method. Applied Physics Express, 2012, 5, 125104.	2.4	2
134	Improved photovoltaic response by incorporating green tea modified multiwalled carbon nanotubes in organic–inorganic hybrid solar cell. Canadian Journal of Physics, 2014, 92, 849-852.	1.1	2
135	Role of the solvent in large crystal grain growth of inorganic-organic halide FA0.8Cs0.2Pbl <i>x</i> Br3 â`` <i>x</i> perovskite thin films monitored by ellipsometry. Journal of Vacuun Science and Technology B:Nanotechnology and Microelectronics, 2019, 37, .	11.2	2
136	Fabrication of Molecular Crystal Nanostructures by a Selective Growth Method Hyomen Kagaku, 1998, 19, 14-20.	0.0	2
137	Real-Time Ellipsometric Characterization of Initial Growth Stage of Poly(3,4-ethylene) Tj ETQq1 1 0.784314 rgBT / Applied Physics, 2011, 50, 081603.	Overlock 2 1.5	10 Tf 50 34) 2
138	Mist chemical vapor deposition of Al _{1â^'<i>x</i>} Ti <i>_x</i> O <i>_y</i> thin films and their application to a high dielectric material. Journal of Applied Physics, 2022, 131, 105301.	2.5	2
139	Crystalline Silicon/Graphene Oxide Hybrid Junction Solar Cells. Japanese Journal of Applied Physics, 2012, 51, 10NE22.	1.5	1
140	Site-dependence of relationships between photoluminescence and applied electric field in monolayer and bilayer molybdenum disulfide. Japanese Journal of Applied Physics, 2019, 58, 015001.	1.5	1
141	State-of-the-Art of Solution-Processed Crystalline Silicon/Organic Heterojunction Solar Cells: Challenges and Future. Challenges and Advances in Computational Chemistry and Physics, 2021, , 33-56.	0.6	1
142	Surface Modification of Poly(3,4-ethylene dioxthiophene):Poly(styrene sulfonic acid) (PEDOT:PSS) Films by Atmospheric-Pressure Argon Plasma for Organic Thin-Film Solar Cells. Journal of Nanoscience and Nanotechnology, 2011, 11, 8035-8039.	0.9	1
143	Comparative Study on Surfaces of Single-Crystalline Substrates. From Dielectric Substance to Semiconductor and Metal. Layered Material Substrates Hyomen Kagaku, 2000, 21, 716-723.	0.0	0
144	Low-energy electron energy loss spectroscopy of monolayer and thick La@C[sub 82] films grown on MoS[sub 2] substrates. AIP Conference Proceedings, 2001, , .	0.4	0

Keiji Ueno

#	Article	IF	CITATIONS
145	Increased Organic Photovoltaic Cell Efficiency by Incorporating a Nonionic Fluorinated Surfactant Cathode Interlayer. Applied Physics Express, 2012, 5, 121601.	2.4	0
146	Solution-Processed Organic/Crystalline-Silicon Heterojunction Solar Cells with Improved Light-Induced Stability. , 2015, , .		0
147	van der Waals junctions of layered 2D materials for functional devices. , 2015, , .		0
148	Exciton Diffusion in hBN-encapsulated Monolayer MoSe2. , 2019, , .		0
149	Fabrication of Organic/inorganic Hybrid CMOS Devices using Solution-processed Graphene Electrodes. IEEJ Transactions on Electronics, Information and Systems, 2015, 135, 156-159.	0.2	0